Electronic Supplementary Material (ESI) for Journal of Materials Chemistry B.

Magnetic hyperthermia induces effective and genuine immunogenic tumor cell death with respect to exogenous heating

Bin Yan,[#a] Chen Liu,[a] Siyao Wang,[a] Hugang Li,[a] Ju Jiao,[#b] Wee Siang Vincent Lee,[c] Song Zhang,[d] Yayi Hou,[e] Yuzhu Hou,[f] Xiaowei Ma,[g] Haiming Fan,[a] Yi Lv,[h] and Xiaoli Liu*[a,h]

[a] Laboratory of Resource Biology and Biotechnology in Western China, Ministry of Education; Provincial Key Laboratory of Biotechnology of Shaanxi Province, Northwest University, Xi'an, Shaanxi 710069, China

E-mail: liuxiaoli@nwu.edu.cn

[b] Department of Nuclear Medicine, The Third Affiliated Hospital of Sun Yat-sen University, 600 Tianhe Road, Guangzhou, Guangdong 510630, China

[c] Department of Materials Science and Engineering, National University of Singapore, 117573, Singapore

[d] College of Life Sciences, Nankai University, Tianjin 300071, China

[e] The State Key Laboratory of Pharmaceutical Biotechnology, Division of Immunology, Medical School; Jiangsu Key Laboratory of Molecular Medicine, Nanjing University, Nanjing, 210093, China

[f] Department of Pathogenic Microbiology and Immunology, School of Basic Medical Sciences, Xi'an Jiaotong University, Xi'an, Shaanxi 710061, China

[g] National Center for Veterinary Drug Safety Evaluation, College of Veterinary Medicine, China Agricultural University, Beijing 100193, China

[h] Institute of Regenerative and Reconstructive Medicine, Med-X Institute, First Affiliated Hospital of Xi'an Jiaotong University, Xi'an, Shaanxi 710049, China; National Local Joint Engineering Research Center for Precision Surgery & Regenerative Medicine, Shaanxi Provincial Center for Regenerative Medicine and Surgical Engineering, First Affiliated Hospital of Xi'an Jiaotong University, Xi'an, Shaanxi 710061, China

Correspondences:

Prof. Dr. X. L. Liu, liuxiaoli@nwu.edu.cn

# These authors contribute equally to this work.

Preparation and characterization of FVIOs

Well-dispersed FVIOs were synthesized based on a previously reported method with slight modifications. The physical properties and magneto-responsive effects of FVIOs were studied. Ferrimagnetic vortex iron oxide nanorings (FVIOs) were fabricated beginning with the hydrothermal synthesis of α-Fe_2O_3 nanorings followed by high-temperature solution-based reduction process to obtain Fe_3O_4 crystalloid phase with ring-shape. Subsequently, phosphorylated mPEG2000 (abbreviated as p-mPEG) was conjugated onto Fe_3O_4 nanorings to afford the water-dispersible. As-obtained Fe_3O_4 nanorings are well-dispersed, presenting a light brown suspension. Scanning electronic microscopy (SEM) images revealed that as-obtained Fe_3O_4 nanorings were ring morphology with an average outer diameter of ~50 nm (Figure S1A). The X-ray diffraction (XRD) analysis of the as-prepared nanorings showed that all peaks could be indexed to cubic inverse spinal structured Fe_3O_4 (JCPDS card, No. 19-0629) (Figure S1C). Fourier transform infrared (FT-IR) spectra were measured for unmodified FVIO, p-mPEG, and phosphorylated mPEG-FVIO (FVIO-PEG). As shown in Figure S1D, both unmodified FVIO and FVIO-PEG have a peak at 575 cm^{-1}, and it could be attributed to the Fe-O bonds in Fe_3O_4. The corresponded peaks in P-mPEG were slightly shifted to 1408, 1277, 1089, and 880 cm^{-1} for the FVIO-PEG, clearly indicating the formation of the presence of p-mPEG on the surface of FVIO.

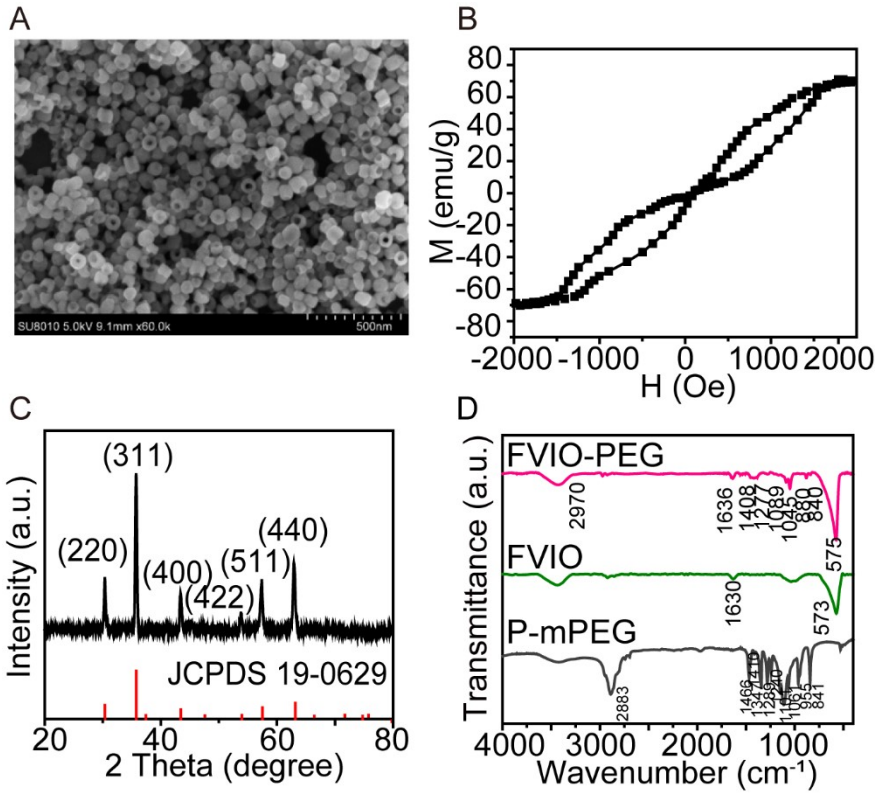

Figure S1 (A) SEM image of FVIOs. (B) Magnetic hysteresis loops of FVIOs. (C) X-ray diffraction patterns of FVIOs. (D) FT-IR spectra of Fe_3O_4 nanorings before ligand exchange, phosphorylated mPEG 2000 and FVIOs after ligand exchange.

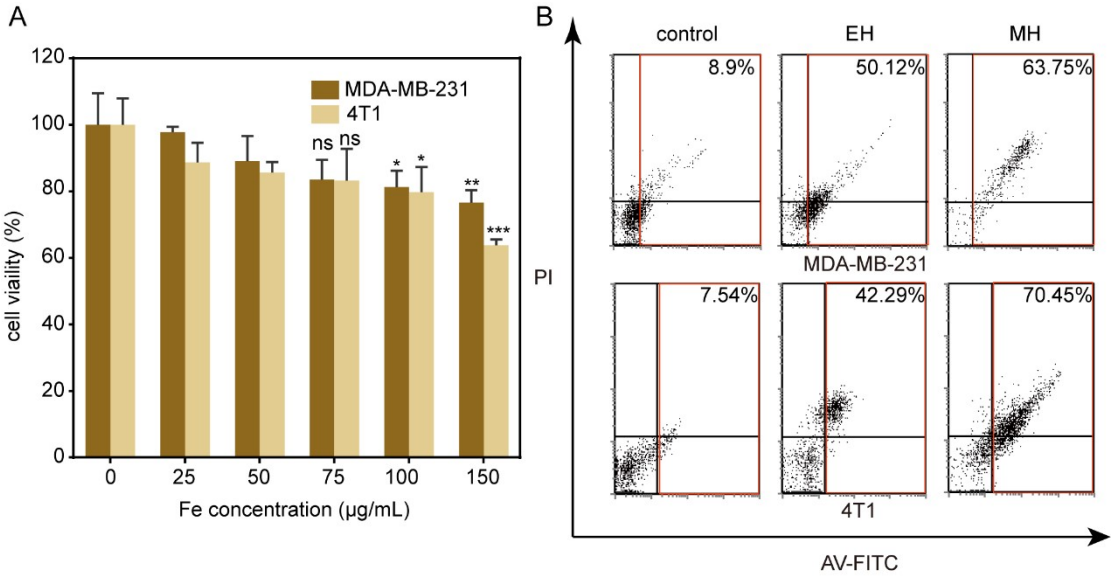

Figure S2 (A) Cell viability of FVIOs. (B) Apoptosis following treatment with MH or water bath heating was measured, using PI/Annexin V labeling and flow cytometry analysis. Statistical analysis was conducted *via* one-way ANOVA with Tukey's multiple comparison tests. The experiments were performed three times independently. To be considered statistically significant, the p-value should be < 0.05. The range of p-values is indicated by the number of the label "*", that is, ****p <0.0001.

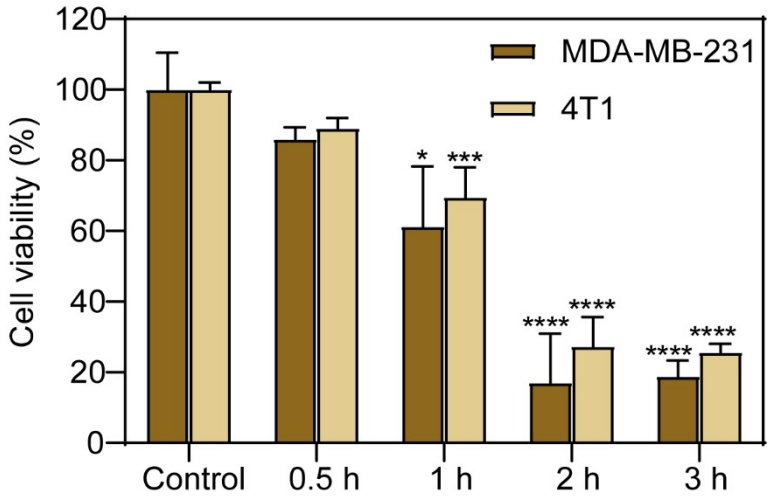

Figure S3 Cell viability of water bath heating treated. Statistical analysis was conducted *via* one-way ANOVA with Tukey's multiple comparison tests. The experiments were performed three times independently. To be considered statistically significant, the p-value should be < 0.05. The range of p-values is indicated by the number of the label "*", that is, *p < 0.1; **p < 0.01; ***p < 0.001; ****p <0.0001. Both cells were exposed to water bath heating (43 ℃) after incubation with FVIOs (75 μg/mL Fe) for different duration time (0.5 h, 1 h, 2 h, and 3 h), a time-dependent cytotoxicity was observed.

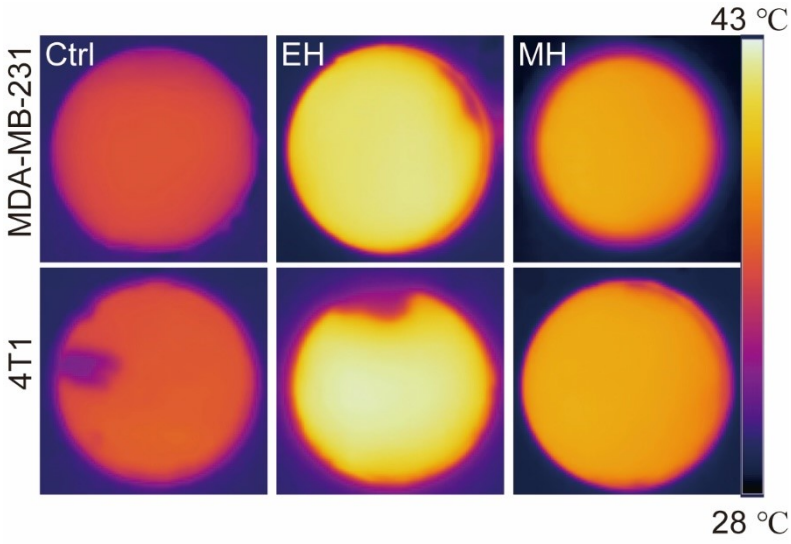

Figure S4 Thermal images acquired by the IR camera of cells at different treatments.

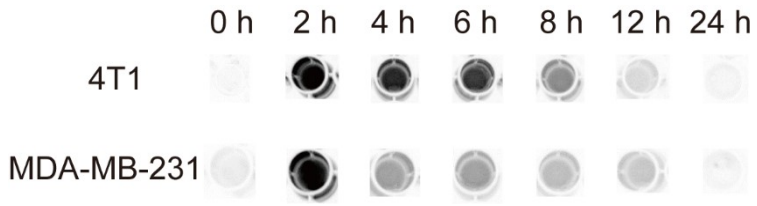

Figure S5 Chemiluminescence images of ATP release after MH treatment.

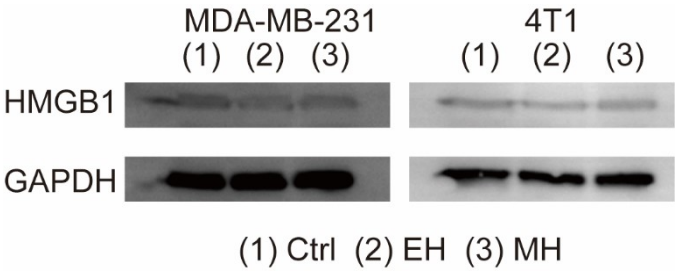

Figure S6 Western blotting detection of HMGB1 expression levels in MDA-MB-231 and 4T1 cells after post-treatment.

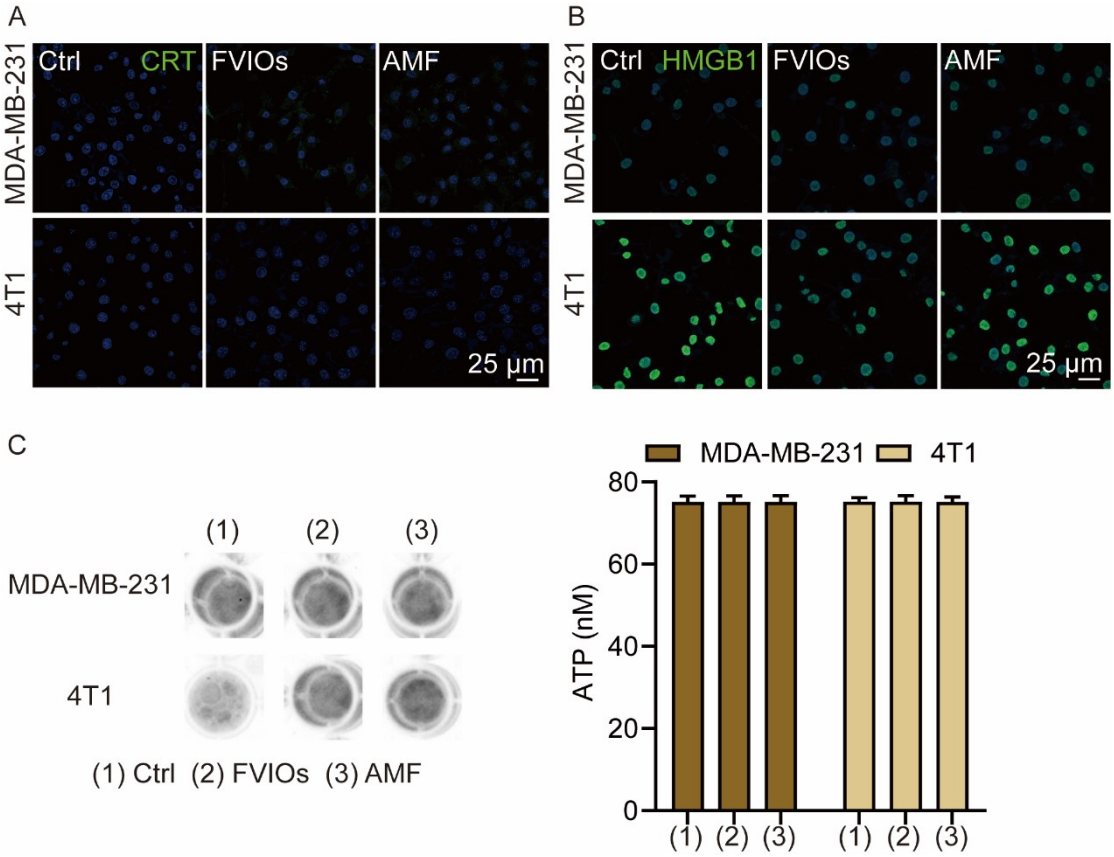

Figure S7 (A) Confocal fluorescence images of both MDA-MB-231 and 4T1 cells after treatment with FVIOs or AMF alone. The cells were stained by CRT-FITC antibody (green) and DAPI (blue) before imaging. Scale bar: 25 μm. (B) Confocal fluorescence images of both MDA-MB-231 and 4T1 cells after treatment with FVIOs or AMF alone. The cells were stained by HMGB1-FITC antibody (green) and DAPI (blue) before imaging. Scale bar: 25 μm. (C) ATP secretions by post-treated MDA-MB-231 and 4T1 cells.

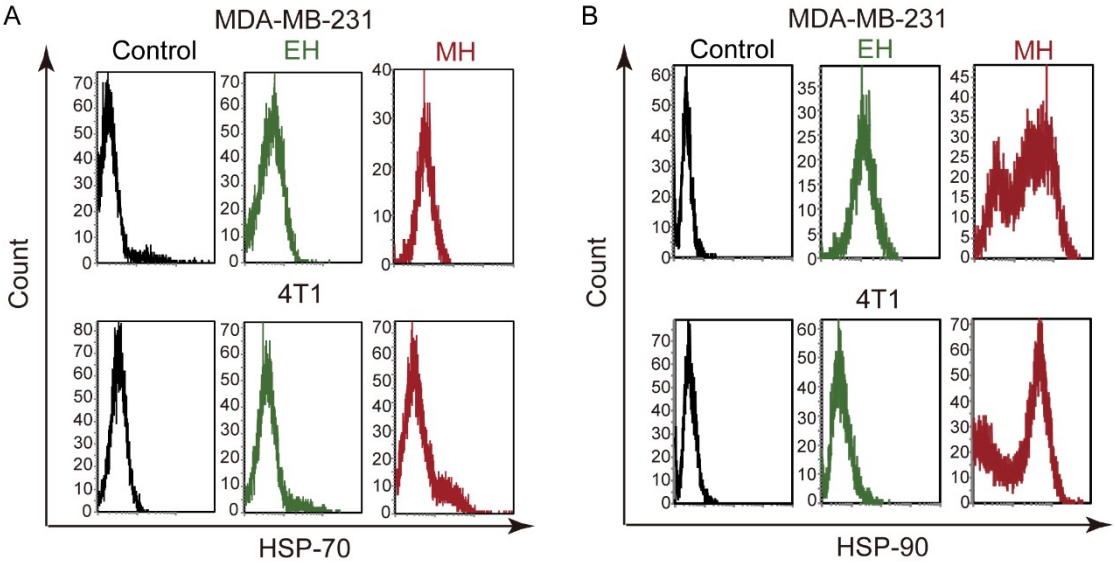

Figure S8 HSP-70/90 release of post-MH or water bath heating treated detected by flow cytometry.

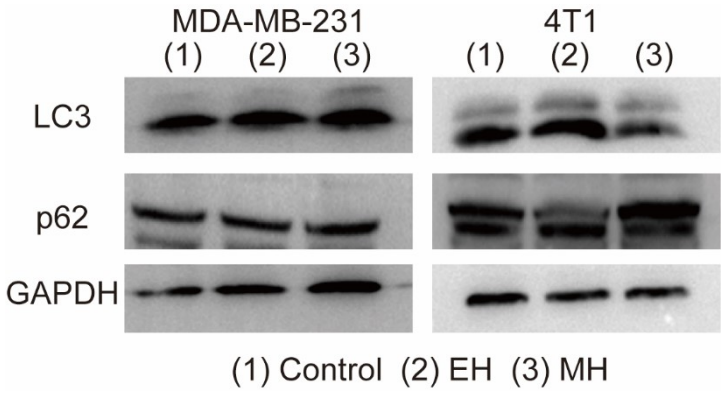

Figure S9 Western blotting detection of LC2 and p62 expression levels in MDA-MB-231 and 4T1 cells after post-treatment.

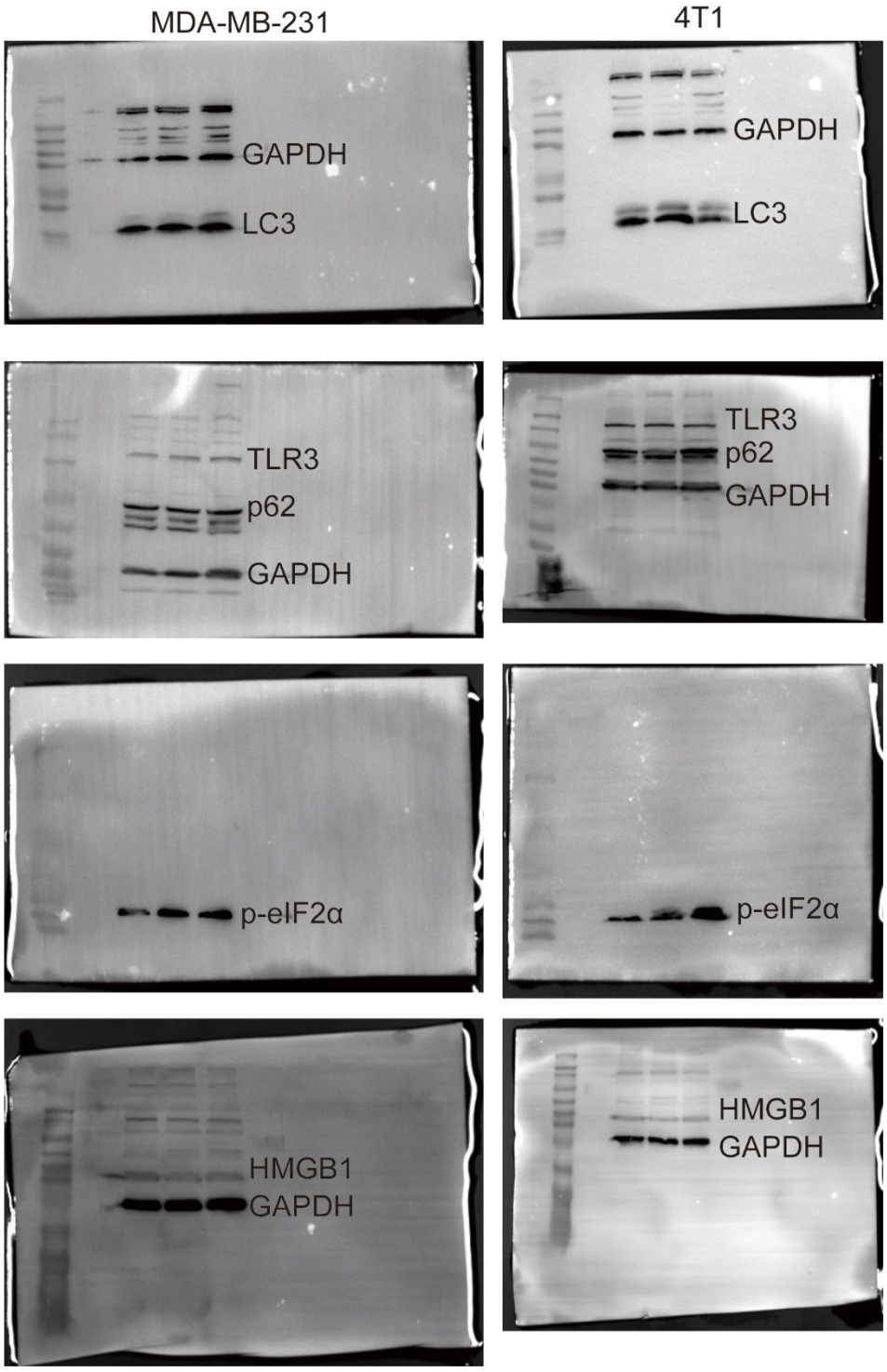

Figure S10 Full uncropped and unprocessed Western Blot data with markers.

Table S1 Characteristics of breast cancer patients in this study

Patients	Age	Type of tumor	Grade
1	34	Invasive ductal carcinoma with intraductal carcinoma	IIB
2	40	Infiltrative ductal carcinoma	IIA
3	49	Infiltrative ductal carcinoma	IIA
4	67	Infiltrative ductal carcinoma	IIIA
5	33	Infiltrative ductal carcinoma	IIB
6	72	Infiltrative ductal carcinoma	IB
7	45	Infiltrative ductal carcinoma	IIA